

COPD lungs show an attached stratified mucus layer that separate bacteria from the epithelial cells resembling the protective colonic mucus

SUPPLEMENTARY TABLES AND FIGURES

Tables S1 – S8, page 1 and separate Excel files

Figure Legends S1 – S9, pages 2 – 5

Figures S1 – S9, pages 6 - 13

Supplementary Tables are given as separate Excel files.

Table S1. Patients from whom BALF samples were collected.

Table S2. Mass spectrometry based proteomics of BALF obtained from human never smoker (n=5) asymptomatic smokers (n=12) and COPD (n=42).

Table S3. Mass spectrometry based absolute quantification of MUC5AC, MUC5B, AGR2, CLCA1, DMBT1, FCGBP, MSLN, MUC1, MUC2, PSCA, TFF3, TGM2 and ZG16B in BALF obtained from human never smoker (n=5) asymptomatic smokers (n=12) and COPD (n=42).

Table S4. Mass spectrometry based proteomics of whole BALF and BALF supernatants (SN) after centrifugation obtained from saline- and PPE-exposed mice.

Table S5. Mass spectrometry based absolute quantification of Muc5ac and Muc5b in whole BALF, BALF supernatants after centrifugation (SN), mucus plugs, and isolated epithelial cells obtained from saline- and PPE-exposed mice.

Table S6. Mass spectrometry based proteomics of isolated airway mucus plugs as stained by Alcian blue and obtained from PPE-exposed mice.

Table S7. Mass spectrometry based proteomics of isolated airway epithelial cells obtained from saline- and PPE-exposed mice.

Table S8. Isotopically labelled peptides used for absolute quantification of human and mouse proteins.

Figure S1. Heat map of the BALF proteome. The localization of some mucus proteins discussed is marked. Never smokers (n=5), asymptomatic smokers (n=12) and chronic obstructive pulmonary disease (COPD) patients (n=42).

Figure S2. Heat map of proteins absolutely quantified with isotopically labelled peptides by mass spectrometry in BALF. Never smokers (n=5), asymptomatic smokers (n=12) and chronic obstructive pulmonary disease (COPD) patients (n=42).

Figure S3. The enzymatic activity of PPE was inactivated by PMSF. (A) Graph showing fluorescence measured every 5 min for 1 h by cleavage of the BODIPY[®] casein substrate as a measure of serine peptidase activity (EnzChek Protease Assay Kit; Invitrogen). Enzymatic activity of PPE was evaluated before and after incubation with 1 mM PMSF overnight at 4°C. PMSF fully inhibited PPE peptidase activity, as the fluorescence signal was equivalent to that measured for a 0.9% saline solution, used as a blank. Results shown are representative of two experiments. Triplicate wells were used for each sample. Mean ± SEM. Two-way repeated measures ANOVA and Tukey's post-test. **** P<0.0001 vs. active PPE. **(B and C)** Low and high magnification images of lungs from mice exposed to inactivated PPE. Scale bar in C, 100 µm.

Figure S4. The distribution of airway mucus obstruction induced by PPE in mice is related to the diameter of the airways. (A) Image showing a transverse section of an airway and the representation of its minimum Feret's diameter (XFmin), defined as the shortest distance between any two parallel tangents on the airway.

Scale bar, 50 μm . **(B)** The XFmin was assessed for each airway section classified depending on its level of obstruction in mice exposed to PPE. Individual data, medians and interquartile ranges. $P < 0.05^*$, $P < 0.01^{**}$ and $P < 0.0001^{****}$ vs. the 10-30 % obstruction range, Kruskal-Wallis with Dunn's post hoc test. **(C)** The same data as in B, but the y-axis was cut at 50 μm to illustrate airways smaller than 50 μm in diameter. **(D)** The correlation between XFmin and obstruction levels was studied both including all airway sections [$r_{(1)}$] or only airway sections with a percentage of obstruction higher than 10 % [$r_{(2)}$]. Two-tailed Spearman's correlation. Each dot represents an airway section. $n=591$ airway sections from 9 animals. **(E)** The same data as in D but the y-axis was cut at 50 μm to illustrate airways smaller than 50 μm in diameter.

Figure S5. Intranasal PPE induced lung inflammation and structural damage.

(A) Transmission electron micrographs showing secretory cells, which in PPE-exposed mice contained electron lucent vesicles and released their content to the airway lumen. Representative of 3 animals/group. Scale bars, 2 μm . **(B)** Formaldehyde fixed paraffin sections stained with H&E revealed alveolar breakdown could be observed in mice challenged with PPE compared with controls instilled with saline. (A and B) Representative of 4-5 animals/group. Scale bars, 100 μm . **(C)** Comparison of cytokine and chemokine levels in BALF from vehicle and PPE-exposed mice, $n = 9-17$ animals/group, data presented as median \pm interquartile range, IL-1 β $P = 0.001^{**}$, IL-4 $P < 0.0001^{****}$, IL-5 $P < 0.0001^{****}$, IL-6 $P = 0.02^*$, KC, TNF α , TARC and MDC $P < 0.0001^{****}$, EGF $P = 0.01^{**}$, Mann-Whitney U test. KC: Keratinocyte-derived chemokine; TARC: Thymus and activation-regulated chemokine; MDC: Macrophage-derived chemokine.

Figure S6. Characterization of isolated mouse airway epithelial cells. (A) Initial percentage of epithelial cells (EpCAM+), leukocytes (CD45+) and neutrophils (Ly-6G+) in a pooled cellular suspension recovered from three mice induced by intranasal administration of LPS. (B and C) Percentage of CD45+ cells and Ly-6G+ cells recovered by magnetic beads and by this depleted from the initial cellular suspension. (D) Purity of the recovered epithelial cellular suspension after the two negative selections removal of CD45+ and Ly-6G+ cells by magnetic beads.

Figure S7. Immunostainings confirm increased production of mucus-related proteins. (A – D) Representative low magnification images of lung sections from vehicle (Saline)- and PPE- exposed mice stained with Muc5b (red; A), Muc5ac (red; B), Clca1 (red; C) and Fcgbp (red; D). Dot plots graphs quantifying the fluorescence intensity of proteins stain expressed as percentage of the mean intensity in saline-exposed mice (taken as 100%). n = 9 animals/group, data presented as median \pm interquartile range, (A) $P = 0.0002^{***}$, (B) $P < 0.0001^{****}$, (C) $P < 0.0001^{****}$, (D) $P = 0.001^{**}$, Mann-Whitney U test. Scale bars, 500 μm . (E) Confocal microscope images showing the colocalization of Muc5ac and Muc5b in the airways after administration of saline (left) or PPE (right). Representative of 4 mice/group. Scale bars, 50 μm . Nuclei are stained blue.

Figure S8. Mucus-related proteins overexpression induced by PPE in mice depends on the proteolytic activity of PPE. (A-F) Representative low magnification images of lung sections from mice exposed to PPE inactivated by

PMSF. Sections were stained for Muc5b (red; A), Muc5ac (red; B), Clca1 (red; C) and Fcgbp (red; D). Scale bars, 500 μ m. Confocal microscope high magnification images showing the overproduction of Clca1 (E) and Fcgbp (F) by airway epithelial cells and their accumulation in mucus plugs after PPE intranasal instillation. Scale bars, 50 μ m. (A-F) Representative of 4-9 animals/group. Nuclei are stained blue.

Figure S9. Immunostaining by Muc5b of lungs of control mice and by Muc5ac on PPE-treated mice followed by treatment with saline or hypertonic saline and the instillation of Pseudomonas bacterial. A) Immunostaining of Muc5b mucin (green) in non-treated animals. Staining of goblet cells is shown, but no mucus layer. Nuclei stained blue. Representative of 3 mice, scale 30 μ m. B) PPE-exposed lungs were instilled with *P. aeruginosa*, BAL was collected after 10 min by instilling 0,8 ml PBS and aspirating it back twice, then the lungs were isolated, fixed in Carnoy and immunostained for Muc5ac (red), *P. aeruginosa* (white), and nuclei (blue). Bacteria are trapped by the mucus and was not removed by washing with PBS. Representative of 3 mice, scale 30 μ m C) PPE-exposed lungs were instilled with *P. aeruginosa*, BAL was collected after 10 min by instilling for two times 0,8 ml hypertonic saline (7%) and aspirating it back after 20 min. Then, the lungs were isolated, fixed in Carnoy and immunostained for Muc5ac (red), *P. aeruginosa* (white), and nuclei (blue). The bacteria are trapped in the stagnated adherent lung mucus that persisted after treatment with 7% hypertonic saline. Representative of 4 mice, scale 30 μ m.

Figure S1

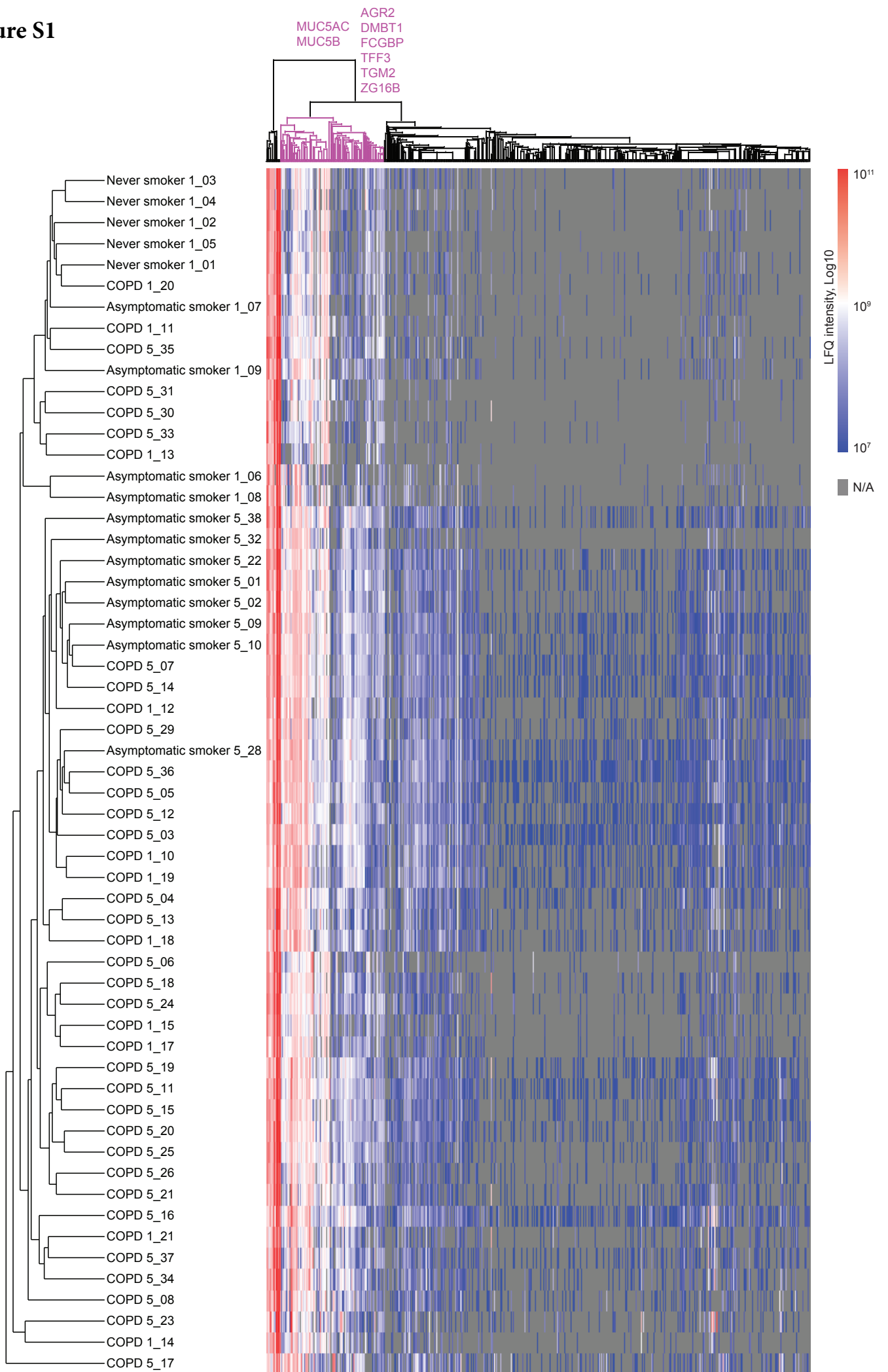


Figure S2

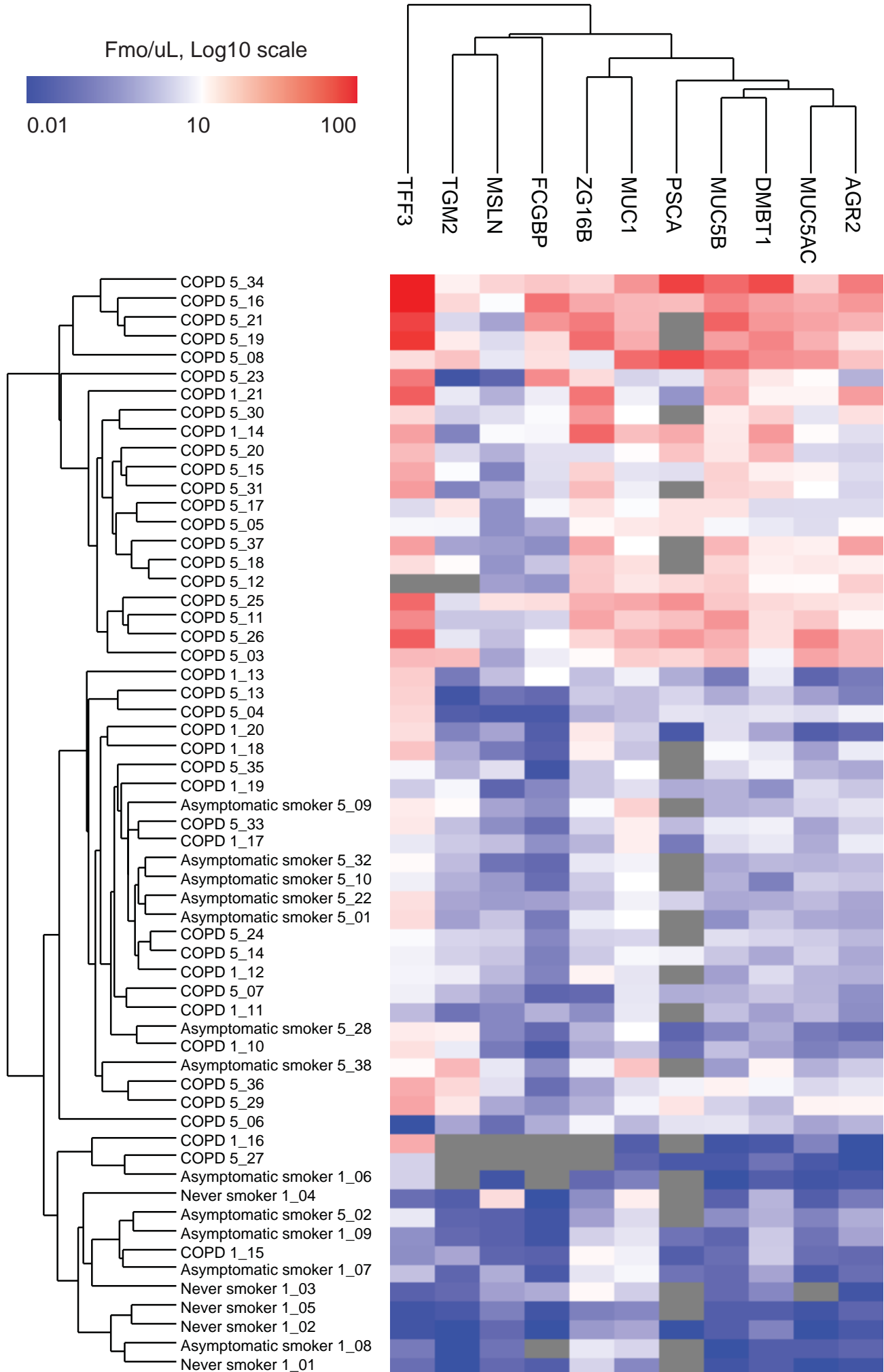


Figure S3

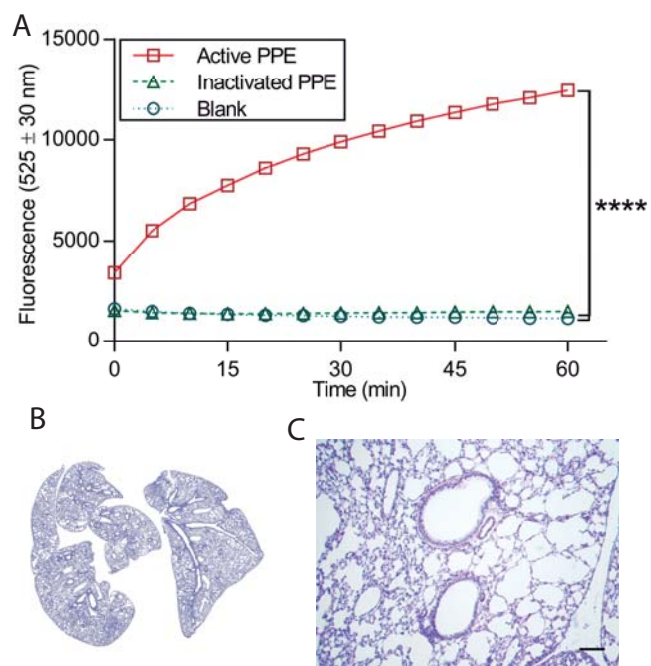


Figure S4

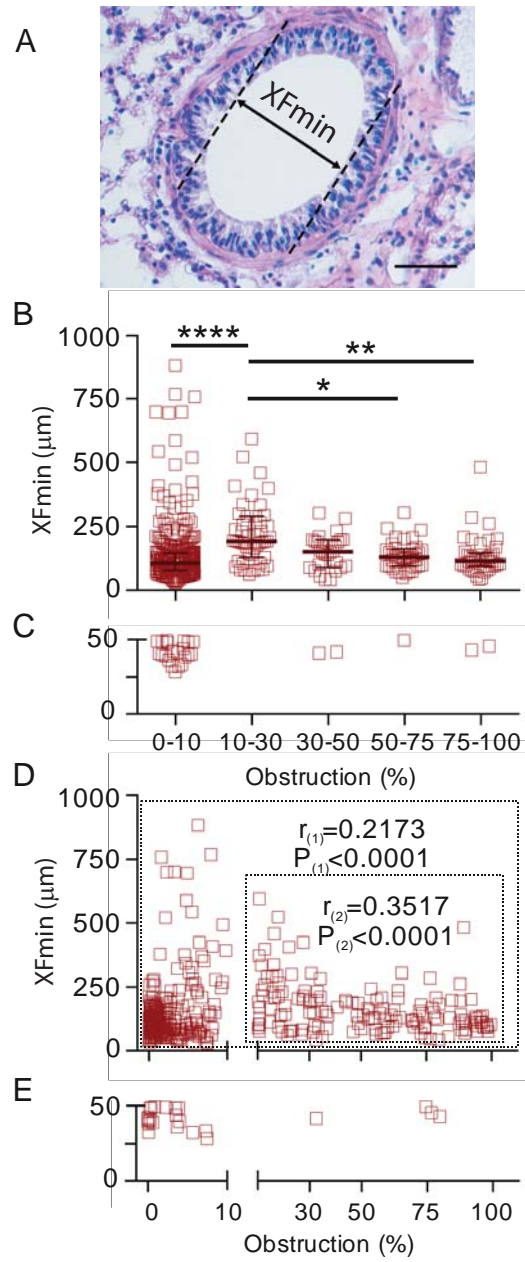


Figure S5

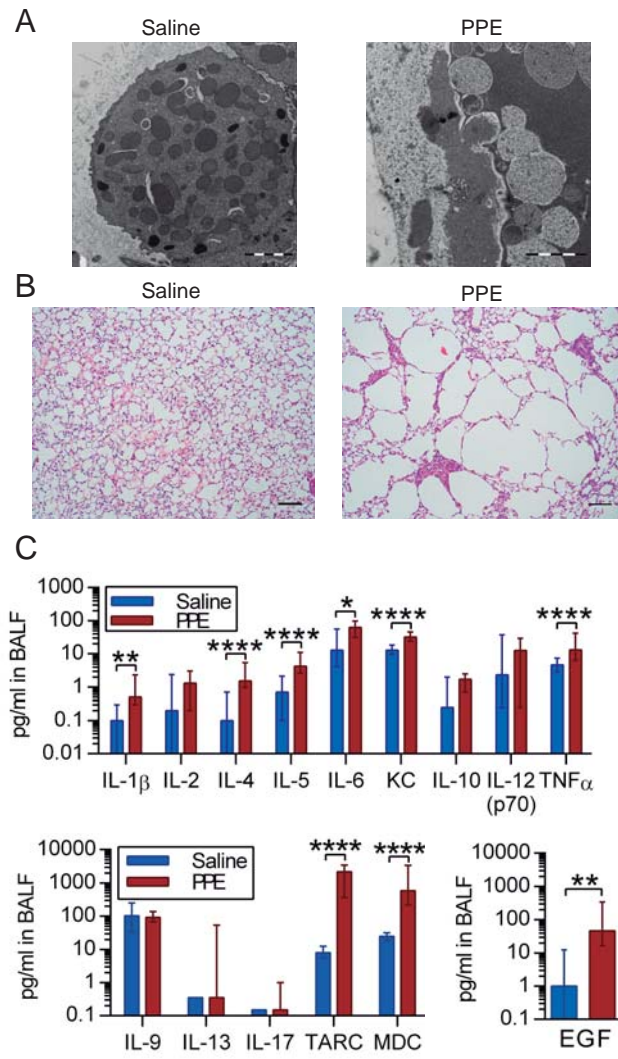
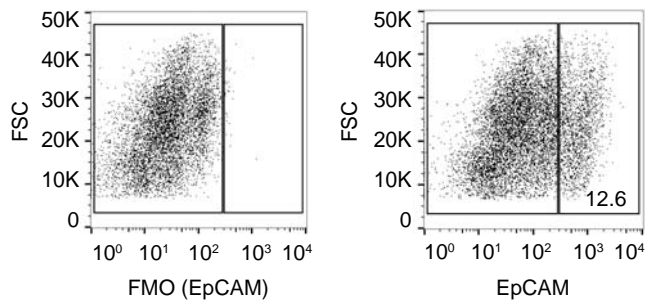
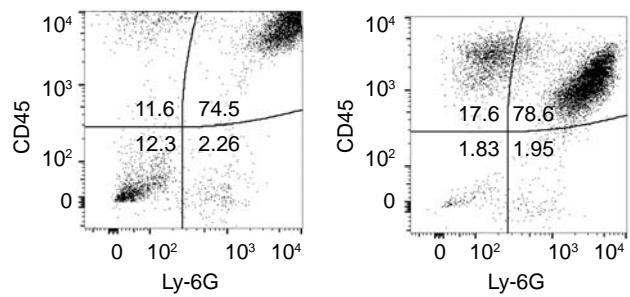


Figure S6

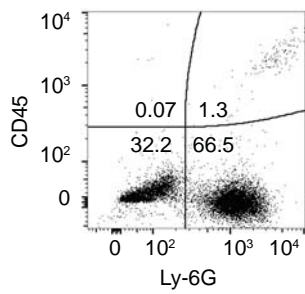
A Airway cellular suspension before depletion of immune cells



B Cellular fraction CD45⁺



C Cellular fraction Ly-6G⁺



D Recovered fraction Ly-6G⁻CD45⁻

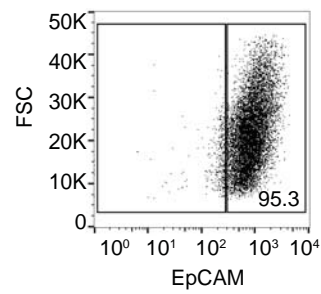
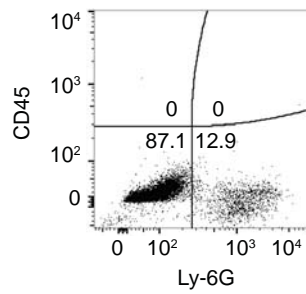


Figure S7

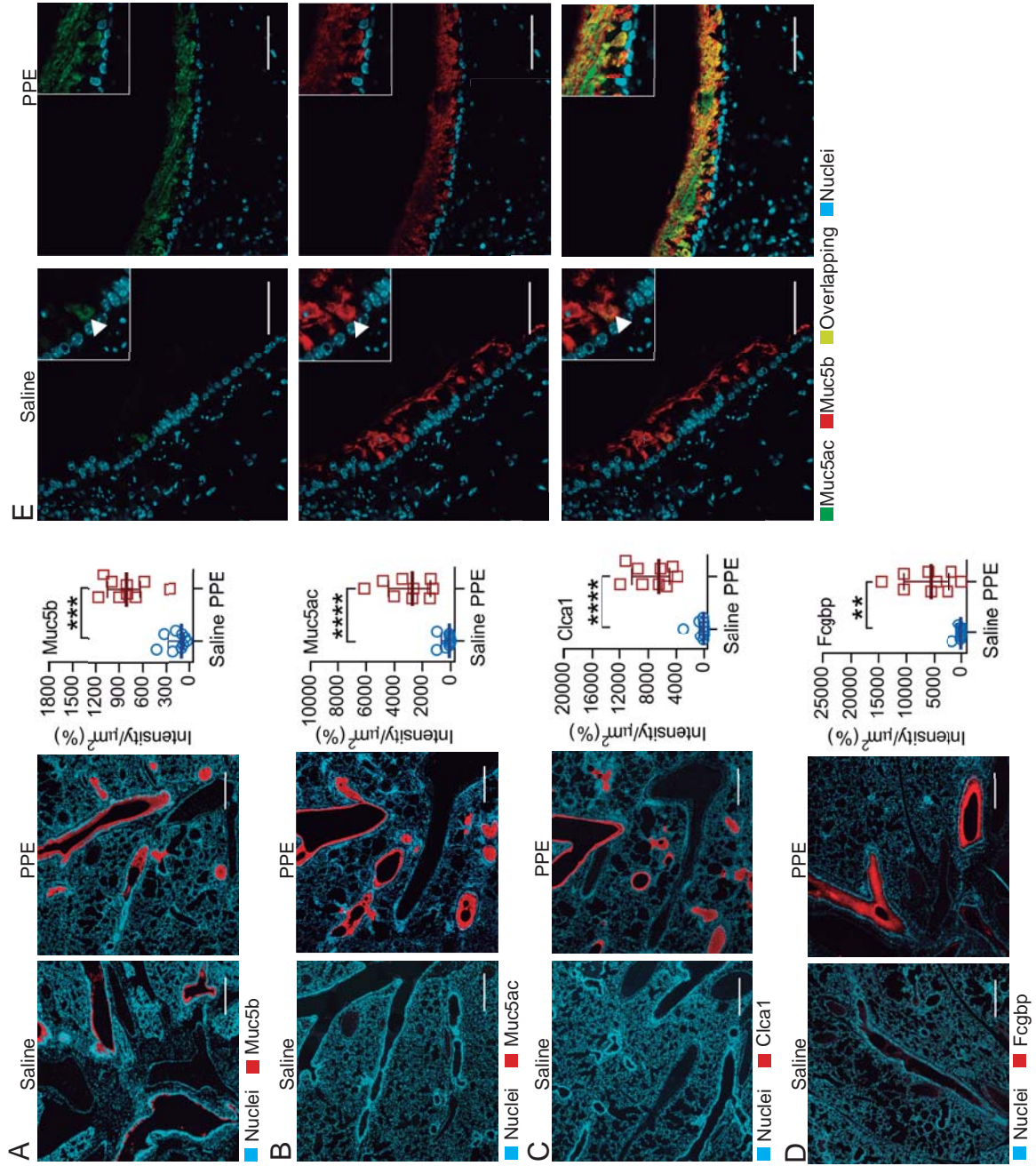


Figure S8

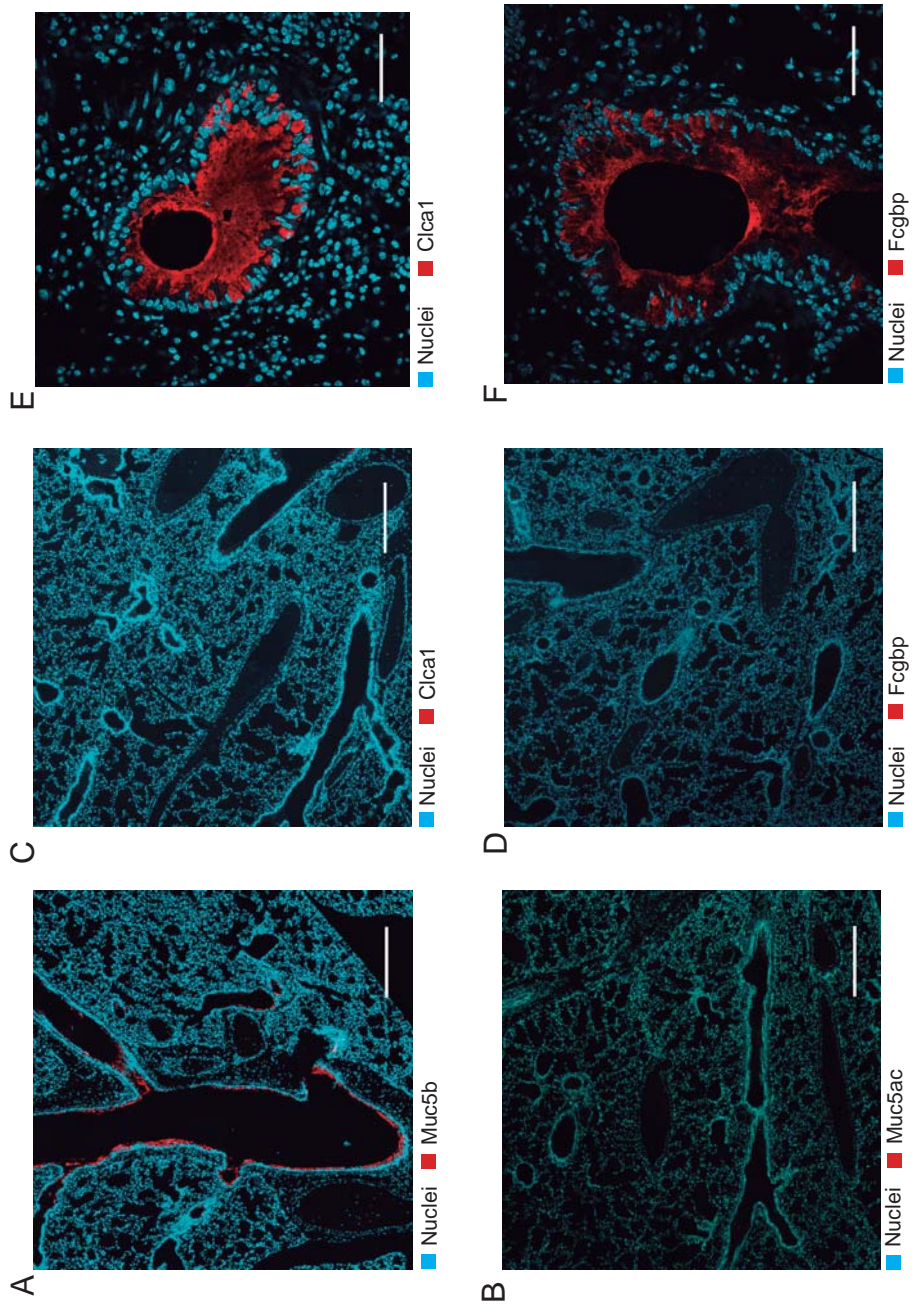


Figure S9

